A Design Study of 4/2 Switched Reluctance Motor Using Particle Swarm Optimization

Winna Phuangmalai[1],
Mongkol Konghirun[2], and **Nattapon Chayopitak**[3], Non-members

ABSTRACT

This paper presents the use of particle swarm optimization (PSO) algorithm applied to the optimal design of the 4/2 switched reluctance motor (SRM). The main advantage of designing 4/2 SRM is the robust rotor structure for high speed unidirectional rotating applications such as the air conditioner's blower. In the designing process, the finite element method magnetics (FEMM) is employed to analyze the designing SRM with its optimized parameters given by PSO. This PSO algorithm is efficient and flexible. The objective function is based on the ripple torque minimization with respect to rotor node position. The PSO algorithm is described and the FEMM simulation results with detailed analysis will be given for verifying optimal rotor design by PSO algorithm.

Keywords: Particle Swarm Optimization, Switched Reluctance Motors , Finite Element Method

1. INTRODUCTION

Nowadays, the switched reluctance motor (SRM) is interested in industrial and home applications such as blowers, pump, vacuum cleaners, compressors, spindle drives, and etc because of its high power density and compact size of a high speed motor [1-2]. The SRM has a simple and strong structure. The rotor is simple and requires relatively few manufacturing steps. It also tends to have low inertia. The stator windings are also simple. The end turns of windings are short and have no phase-phase crossovers. There are no permanent magnets. Therefore, the mechanical structures are resistant to the environment, high temperature and suitable in high speed applications [3-4]. It is well known that the core losses are proportional to the electrical frequency and the switching losses in power semiconductors are proportional to switching frequency. Thus, high electrical frequency operation can cause increasing losses of SRM. For a particular operating rotor speed, the electrical frequency can be reduced when the number of rotor poles is reduced. In order to reduce power losses in high speed drives, the number of rotor poles should be lowest as possible. The choice of 2-poles rotor is thus preferable in high speed drives.

In this paper, the 4/2 SRM was designed for air blower system which requires only one direction of rotation. In order to satisfy the application, variable air gap at the rotor poles is being proposed to improve the torque characteristics of self-starting performance with respect to the rotor designs. This paper is organized as follows. In section 2, the 4/2 SRM design is described. In section 3, the PSO algorithm is explained to optimize the 4/2 SRM. The simulation results are given in section 4 and the conclusion is in section 5.

2. 4/2 SRM DESIGN

Switched reluctance motor consists of stator and rotor, which are made of laminated silicon steel. Fig. 1 shows the 4/2 SRM structure. The winding on the stator consist of two-phase windings. Phase-A stator windings consist of two windings installed in poles A1 and A2. Both A1 and A2 windings are connected in series. Likewise, the same winding configuration is true for phase-B. When the current flows through the phase windings, the rotor tends to align with that stator poles in the direction of minimum reluctance position.

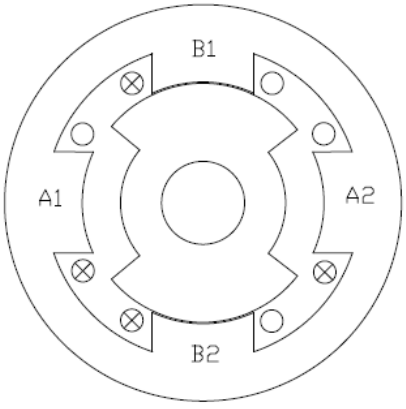

Fig.1: *4/2 switched reluctance motor.*

Manuscript received on April 10, 2013 ; revised on May 9, 2013.

[1,2] The authors are with Department of Electrical Engineering, Faculty of Engineering, King Mongkut's University of Technology Thonburi., E-mail: fah_electrical46@hotmail.com and mongkol.kon@kmutt.ac.th

[3] The author is with National Electronics and Computer Technology Center., E-mail: nattapon.chayopitak@nectec.or.th

To design the proposed SRM, the FEMM is mainly tool. This two-dimensional partial differential solving program has the ability to calculate and analyze the various motor designs. The motor torque characteristics are analyzed by using FEMM. Table 1 shows the specific parameters of two-phase proposed SRM and Table 2 shows its materials for designing.

Table 1: *Parameters of two-phase SRM.*

Parameter	Value
Output power (W)	300
Input voltage (V)	220
Outer diameter of stator (mm)	82
Inner diameter of stator (mm)	44
Stator back iron diameter (deg)	65.5
Shaft diameter (mm)	13.2
Length of axial stack (mm)	40
Pole arc of stator (deg)	48
Pole arc of rotor (deg)	102
Rotor inner diameter (mm)	26.2
Length of air gap (mm)	0.25
Winding turns per pole	100

Table 2: *Material of two-phase SRM.*

Type	Material
Stator	M-19 Steel
Rotor	M-19 Steel
Wire	Copper 22 SWG

3. PARTICLE SWARM OPTIMIZATION ALGORITHM AND FINITE ELEMENT METHOD MAGNETICS

The optimal design of SRM uses a particle swarm optimization (PSO) algorithm and finite element method magnetics. The PSO is used to search the optimal design parameters by maximizing the fitness function. The FEMM is used as a solver of the fitness function.

The PSO algorithm is a population based on stochastic optimization strategy which was developed in 1995 by Kennedy and Eberhart [5]. They were inspired by the social behaviour of a flock of birds, a group of ants, a school of fish, etc. Firstly, the system has a population of solution that are random. Each potential solution called "particle". Each particle is given a random velocity. The particles have memory and tracking the best previous position (P_{best}) and the particle with the greatest fitness is called the global best (G_{best}) of the swarm. The basic concept of PSO algorithm is to accelerate the particle to P_{best} and G_{best} by accelerating the weights randomly in each step.

The main steps in PSO and the selection process are explained below:

a) Initialize the population with random position and velocity of particle in space of problem.
b) Evaluate the fitness of each particle in the swarm.
c) For each iteration, it compares the fitness of each particle with P_{best} obtained. If the current value is better than P_{best}, then set the current value equal to P_{best}.
d) Compare P_{best} of the particle with one another and update the swarm global best location with Gbest.
e) Change the velocity and position of the particle according to equations (1) and (2), respectively.

$$V_i = \omega \times V_i + rand_1(P_i - X_i) + C_2 \times rand_2(P_g - X_i) \quad (1)$$

$$X_{i+1} = X_i + V_i \quad (2)$$

PSO has many parameters and these are described as follows: V_i and X_i present the velocity and position of the i^{th} particle. The P_i and P_g are the local best position and the global best position, respectively. The $rand_1$ and $rand_2$ are two uniform random functions. The c_1 and c_2 are the acceleration coefficients, and ω is the inertia weight, which is chosen beforehand.

The process is repeated until total generation number is reached. The modeling 4/2 SRM to be optimized is shown in Fig. 2. In the optimal design, a constant value of the inertia weight $\omega = 0.9$, acceleration coefficients $c_1 = 0.12$ and $c_2 = 1.2$, and maximum iteration = 20. The PSO algorithm is used to find the current position (X_i) at node to be optimized. Then, the ripple torque is calculated by FEMM.

The fundamental physical equations in (3)-(5) that describe the electromagnetic fields are given by Maxwell's equations. These equations are always solved by using vector potential formulation.

$$\nabla \cdot B = 0 \quad (3)$$

$$\nabla \times E = -\frac{dB}{dt} \quad (4)$$

$$\nabla \times H = J \quad (5)$$

These equations are presented in terms of vector field variables E, B and H.

In equation (6), the magnetic vector field B is presented in term of the vector potential as:

$$B = \nabla \times A \quad (6)$$

The relationship between H and B is shown in equation (7):

$$H = r.B \quad (7)$$

where r is inverse of the permeability. The vector potential equation for magnetic field in equations (6)

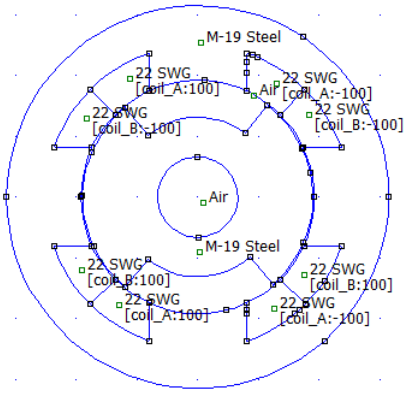

Fig.2: *Modelling 4/2 SRM by FEMM.*

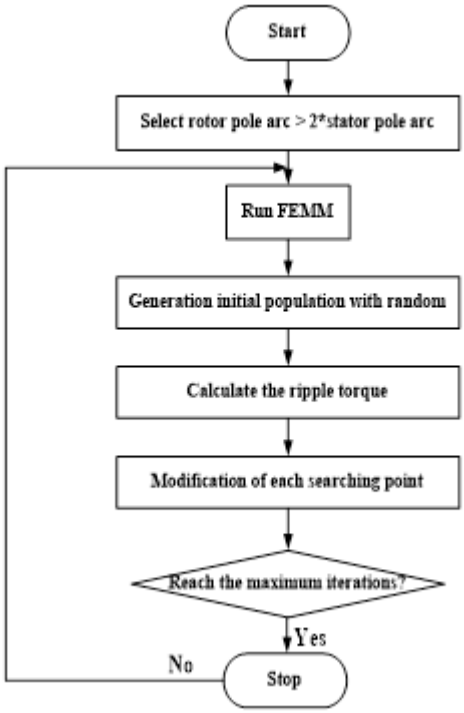

Fig.3: *Flow chart of the optimal design using FEMM and PSO.*

and (7) replaced to equation (5). It shows in equation (8).

$$\nabla \times (r \cdot \nabla \times A = J) \tag{8}$$

In this paper, the FEMM version 4.2, the open source software, is mainly used. A powerful scripting language, Lua 4.2, is integrated with the program. Lua allows users to create batch runs, describe geometries parametrically, perform optimization, and etc. Lua is also integrated into every edit box in the program so that formulas can be entered in lieu of numerical values, if desired [6]. Overall optimizing flow chart is shown on Fig. 3.

The objective function that is selected to be minimize is the ripple torque as shown in equation (9)

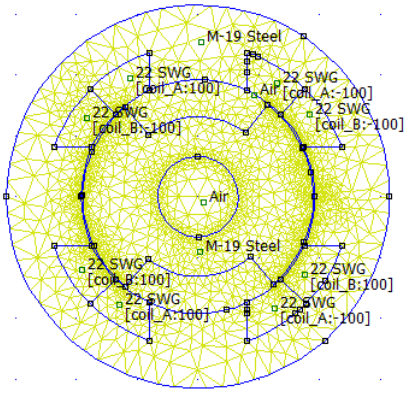

Fig.4: *FEMM mesh of 4/2 SRM.*

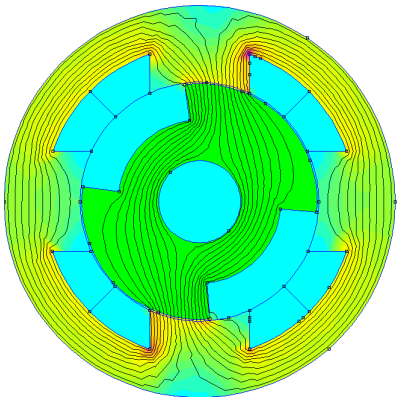

Fig.5: *Flux distribution of 4/2 SRM.*

$$T_{rip} = \frac{T_{max} \times T_{avg}}{T_{avg}} \times 100 \tag{9}$$

Many parameters are described as follows: T_{rip} is the ripple torque. T_{max} is the maximum torque and T_{avg} is the average torque.

The mesh of designing 4/2 SRM by FEMM is shown in Fig. 4. After simulating, the flux distribution of 4/2 SRM can be illustrated in Fig. 5.

4. SIMULATION RESULTS

In this section, the simulation results are presented into two subsections. In the first subsection, the simulation results of the minimizing ripple torque by using PSO are given. Secondly, the simulation results related other aspects such as the starting torque, the maximum torque, and the winding turns per pole are investigated.

4.1 The minimizing ripple torque

The ripple torque was previously defined in equation (9). It is basically calculated by the difference between the maximum torque and the minimum torque with respect to the average torque. This subsection

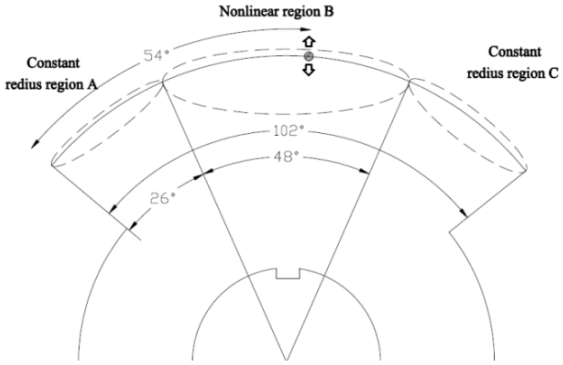

Fig.6: *Regions of rotor surface showing the node to be optimized.*

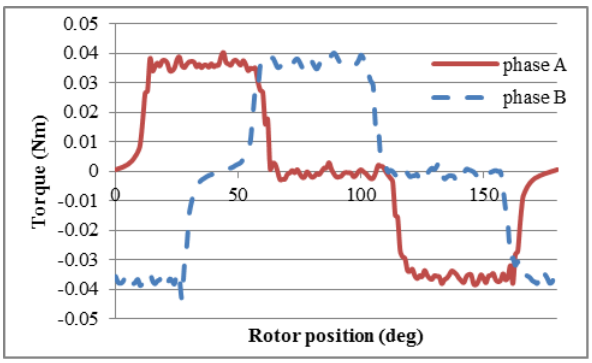

Fig.7: *Torque of 4/2 SRM by using PSO.*

discusses the reduction of the ripple torque by using PSO. Fig. 6 shows three different rotor surface regions; i.e., constant radius regions A, nonlinear region B and constant radius regions C. The node at 54 degree on nonlinear region B will be primarily focused on optimization.

Referring to Fig. 6, the node at 54 degree on nonlinear region B is moved in the direction of the y-axis. The values of parameters are already given from Table 1. The simulation results of two phase torques versus rotor position when using PSO is shown in Fig. 7 and the lengths of air gap before and after optimization are summarized in Table 3. Fig 8 shows the rotor structure with optimized air gap at 54 degree node. After running PSO, the length of air gap for 4/2 SRM is converging to 0.39 mm, giving the minimum ripple torque as shown in Fig 9. In Fig. 10, the ripple torque versus iteration is shown. It is clearly that the ripple torque is minimizing as iteration proceeds. According to this result, the ripple torque of optimized node is equal to about 8.36% which is less than the ripple torque of non-optimized node shown in Fig. 11 in which the ripple torque is equal to 13.83%.

Fig.12 shows the comparison of torque between before optimization of rotor shape versus optimal rotor shape using PSO. Clearly, the optimal rotor shape provides improvement of the ripple torque.

Table 3: *Length of air gap at 54 degree node.*

Before optimization	0.20 mm
PSO	0.39 mm

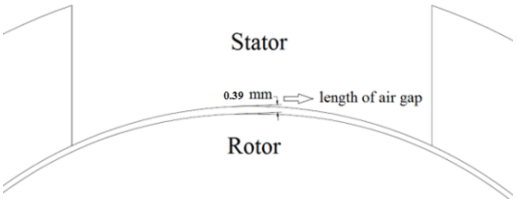

Fig.8: *Length of air gap after optimization.*

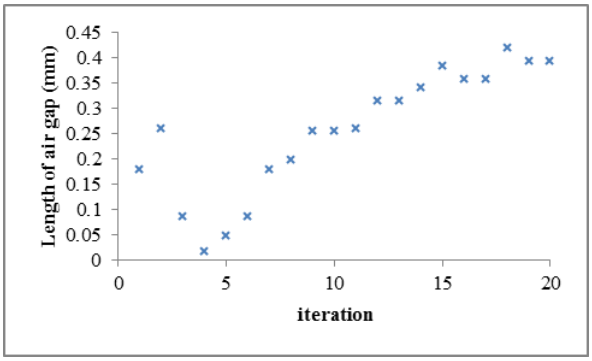

Fig.9: *Length of air gap vs iteration.*

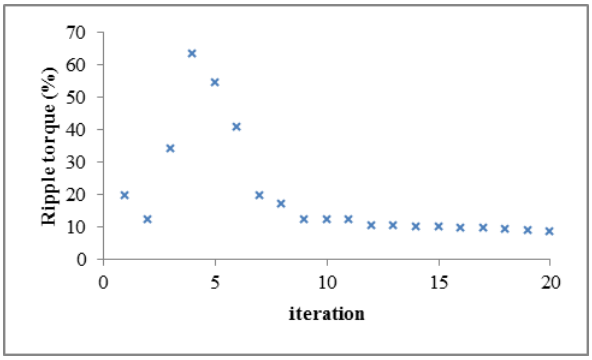

Fig.10: *The ripple torque vs iteration.*

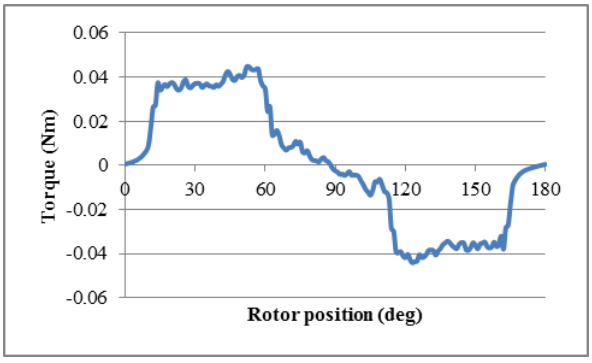

Fig.11: *Torque of non-optimized node.*

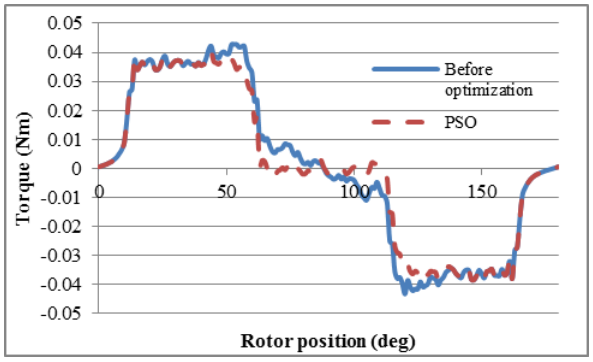

Fig. 12: *Torque before optimization and PSO.*

4.2 Evaluations of optimized SRM

In this subsection, firstly, the adjustment of the pole arc of rotor affecting the starting torque is tested. Secondly, the adding and reducing the winding turns per pole affecting the torque are investigated.

4.2.1 The starting torque

This subsection discusses the simulation results for adjusting the pole arc of rotor, comparing with the pole arc of stator that affects the starting torque characteristics. Table 4 shows the various pole arcs of stator and rotor. Firstly, the simulation result of torque waveform versus rotor position when the pole arc of rotor is longer than the pole arc of stator can be seen in Fig.11. The torque is initially increased from the rotor position of 14 degree, approximately. The maximum torque is around 0.042 Nm. On the other hand, when the pole arc of rotor is shorter than the pole arc of stator as shown in Fig. 13, the simulation result of torque waveform can be seen in Fig.14. In this case, the torque is initially increased from the rotor position of 50 degree. The maximum torque is around 0.048 Nm. Thirdly, when the pole arc of rotor is equal to the pole arc of stator as seen in Fig. 15, the simulation results of torque waveform is shown in Fig.16. The torque is initially increased from starting the rotor position of 30 degree. The maximum torque is about 0.09 Nm. Therefore, the starting torque characteristic can be affected when the pole arc of rotor is adjusted.

Table 4: *Pole arc of stator and rotor.*

Pole arc of stator (degree)	Pole arc of rotor (degree)
48	102 mm
48	48 mm
48	30 mm

4.2.2 The winding turns per pole

This subsection considers the effects of different winding turns per pole. The winding turns per pole

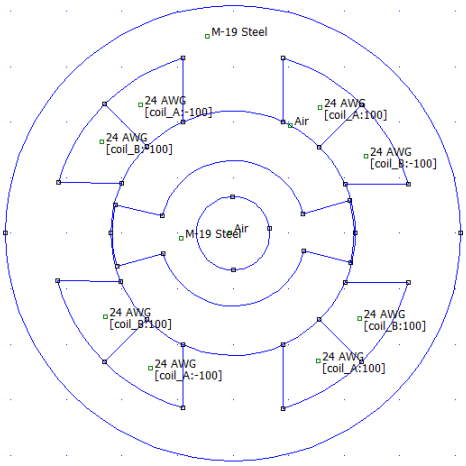

Fig. 13: *Modeling of 4/2 SRM when the pole arc of rotor is shorter than the pole arc of stator*

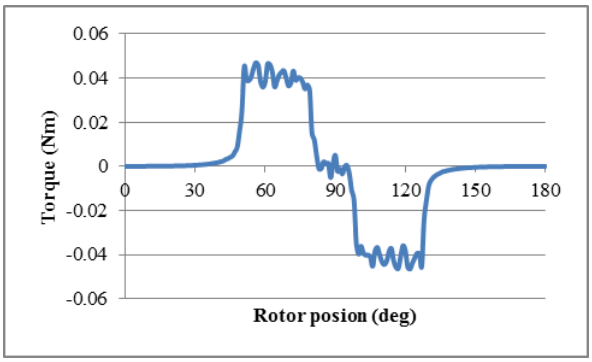

Fig. 14: *Torque of 4/2 SRM when the pole arc of rotor is shorter than the pole arc of stator.*

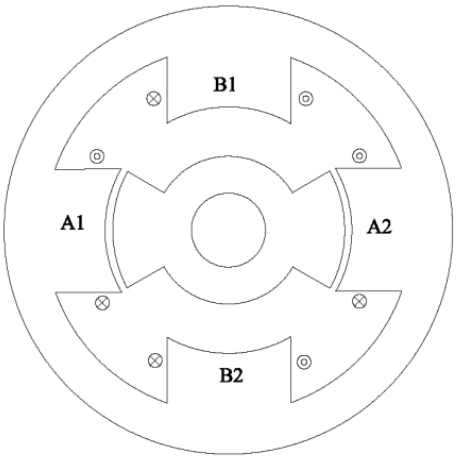

Fig. 15: *Modeling of 4/2 SRM when the pole arc of rotor is equal to the pole arc of stator.*

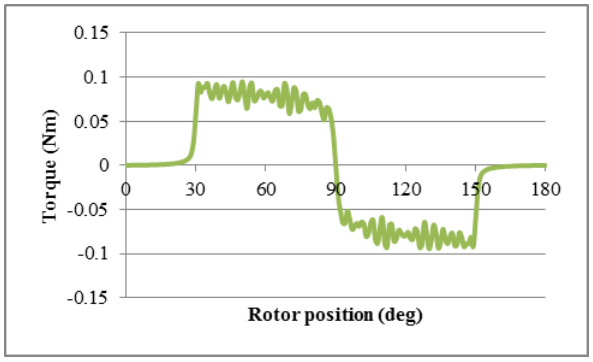

Fig.16: *Torque of 4/2 SRM when the pole arc of rotor is equal to the pole arc of stator.*

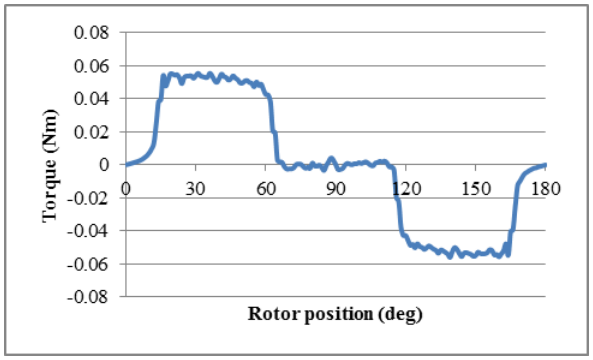

Fig.17: *Torque with winding turns per pole of 120 turns.*

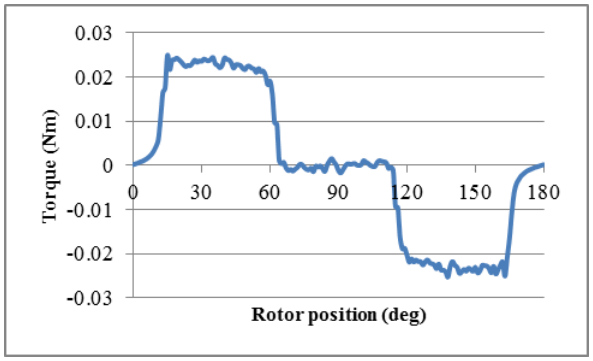

Fig.18: *Torque with winding turns per pole of 80 turns.*

are adjusted to be 80 and 120 turns, comparing with 100 turns. Fig.17 shows the torque produced by 4/2 SRM with the winding turns per pole of 120 turns. Clearly, the torque is increased from one produced by winding turns per pole of 100 turns shown in Fig.7. On the other hand, Fig.18 shows the torque produced by 4/2 SRM with the winding turns per pole of 80 turns. It is expected to observe the lower torque with lower number of winding turns. Referring to these Figs.17 and 18, Table 5 summarizes the torque produced by different winding turns per pole.

Table 5: *Torque produced by different winding turns per pole.*

Winding turns per pole	Torque (Nm)
80	0.023
100	0.035
120	0.054

4.2.3 The phase current

Next, the torque production due to the increase of phase current from 1.0 to 2.5 A is simulated as shown in Fig.19. As expected, the maximum torque is increased from 0.037 to 0.24 Nm with the increase of phase current from 1.0 to 2.5 A, respectively.

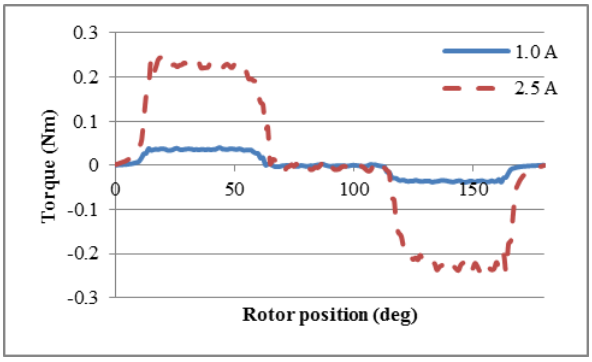

Fig.19: *Torque with the phase current of 1.0A and 2.5A.*

5. CONCLUSION

This paper presents a study design of 4/2 SRM using PSO, optimizing the rotor pole shape for minimizing ripple torque. According to simulation results, the ripple torque can be reduced by 8.36%. with optimized 54 degree node of rotor pole. When the pole arc of rotor is equal to the pole arc of stator, the maximum torque is highest, comparing with the shorter and longer pole arc of rotor. However, in this case of equal pole arc of rotor and stator, the initial torque is generated at rotor position of 30 degree, which may not provide the continuous two phase torque. Both increasing number of winding turns per pole and increasing phase current similarly result in the increased maximum torque of 4/2 SRM.

6. ACKNOWLEDGEMENT

The financial support from Thailand graduate institute of science and technology (TGIST) is acknowledged. The student scholarship recipient code is the TG-44-20-53-061M.

References

[1] K.J. Binns, P.J. Lisboa and M.S.N. AL-Din, "The Use of Canned Rotors in High Speed Per-

manent Magnet Machines," *Int. Conf. Elect. Mach. Drives*, London, England, 1991, pp. 21-25.

[2] Ikeda, M.; Sakabe, S.; Higashi, K. "Experimental study of high speed induction motor varying rotor core construction," *IEEE Trans. Energy Convers.*, vol. 5, iss. 1, pp.98-103, Mar. 1990.

[3] T. Genda, H. Dohmeki, "Characteristics of 4/2 Switched Reluctance Motor for a high speed drive by the excitation angle," *Int. Conf. Elect. Mach. Syst.*, Tokyo, Japan, 2009, pp.1-6.

[4] S. Kozuka, N. Tanabe, J. Asama, A. Chiba, "Basic characteristics of 150,000 r/min switched reluctance motor drive", *Power and Energy Soc. General Meeting-Conver. Delivery Elect.*, Pittsburgh, United States of America, 2008, pp. 1-4.

[5] J. Kennedy, R.C. Eberhart, "Particle swarm optimization," *IEEE Int. Conf. on Neural Netw.*, Piscataway, United States of America, 1995, pp. 1942-1948.

[6] David Meeker, "Finite Element Method Magnetics," User's Manual: Oct 16, 2010.

Winna Phuangmalai received a B.Eng in Electrical Engineering from King Mongkut's University of Technology Thonburi in 2009. Presently, she is studying a master's degree in in electrical engineering at King Mongkut's University of Technology Thonburi. Her research interests electric motor drives.

Mongkol Konghirun received a B.Eng in Electrical Engineering from King Mongkut's University of Technology Thonburi, Thailand in 1995. And he received M.Sc. and Ph.D. degrees in Electrical Engineering from the Ohio State University, USA in 1999 and 2003, respectively. Presently, he is an Assistant Professor with the Department of Electrical Engineering, King Mongkut's University of Technology Thonburi. His research interests include electric motor drives and renewable energy.

Nattapon Chayopitak received the B.S. degree from Columbia University, New York, in 2001, and the M.S. and Ph.D. degrees from Georgia Institute of Technology, Atlanta, in 2003 and 2007, respectively, all in electrical engineering. Presently, he is a Research Engineer with the National Electronics and Computer Technology Center (NECTEC), Industrial Control and Automation Laboratory, Pathumthani, Thailand. His research interests are in design and control of electric drives and manufacturing automation.